2018

Integrated Dynamics Control and Energy Efficiency Optimization for Overactuated Electric Vehicles

Boyuan Li
University of Wollongong, bl995@uowmail.edu.au

Haiping Du
University of Wollongong, hdu@uow.edu.au

Weihua Li
University of Wollongong, weihuali@uow.edu.au

Bangji Zhang
Hunan University, bangjizhang@hnu.edu.cn

Integrated Dynamics Control and Energy Efficiency Optimization for Overactuated Electric Vehicles

Abstract

A large number of studies have been conducted on the dynamics control of electric vehicles or on the optimization of their energy efficiency but few studies have looked at both of these together. In this study, an integrated dynamics control and energy efficiency optimization strategy is proposed for overactuated electric vehicles, where the control of both longitudinal and lateral dynamics is dealt with while the energy efficiency is optimized. First, considering the trade-off between control performance and energy efficiency, criteria are defined to categorize the vehicle motion status as linear pure longitudinal motion and non-linear motion or turning motion. Then different optimization targets are developed for different motion status. For the pure linear longitudinal motion and cornering motion, the energy efficiency and vehicle dynamics performance are equally important and a trade-off control performance between them needs to be achieved. For the non-linear turning motion, vehicle handling and stability performance are the primary concerns, and energy efficiency is a secondary target. Based on the defined targets, the desired longitudinal and lateral tyre forces and yaw moment are then optimally distributed to the wheel driving and steering torques. Finally numerical simulations are used to verify the effectiveness of the proposed strategies. The simulation results show that the proposed strategies can provide good dynamics control performance with less energy consumption.

Disciplines

Engineering | Science and Technology Studies

Publication Details

Li, B., Du, H., Li, W. & Zhang, B. (2018). Integrated Dynamics Control and Energy Efficiency Optimization for Overactuated Electric Vehicles. Asian Journal of Control, 20 (6), 1-15.

Integrated dynamics control and energy efficiency optimisation for over-actuated electric vehicles

Boyuan Li[1], Haiping Du[1], Weihua Li[2] and Bangji Zhang[3]
1. School of Electrical, Computer and Telecommunications Engineering, University of Wollongong, Wollongong, NSW 2522, Australia
2. School of Mechanical, Material and Mechatronic Engineering, University of Wollongong,
Wollongong, NSW 2522, Australia
3. State Key Laboratory of Advanced Design and Manufacturing for Vehicle Body, Hunan University, Changsha 410082, China

Abstract:

A large number of studies have been conducted on the dynamics control of electric vehicles or on the optimisation of their energy efficiency but few studies have looked at both of these together. In this study, an integrated dynamics control and energy efficiency optimisation strategy is proposed for over-actuated electric vehicles, where the control of both longitudinal and lateral dynamics is dealt with while the energy efficiency is optimised. First, considering the trade-off between the control performance and energy efficiency, criteria are defined to categorise the vehicle motion status as linear pure longitudinal motion and non-linear motion or turning motion. Then different optimisation targets are developed for different motion status. For the pure linear longitudinal motion and cornering motion, the energy efficiency and vehicle dynamics performance are equally important and a trade-off control performance between them need to be achieved. For the non-linear turning motion, the vehicle handling and stability performance are the primary concerns, and energy efficiency is a secondary target. Based on the defined targets, the desired longitudinal and lateral tyre forces and yaw moment are then optimally distributed to the wheel driving and steering torques. Finally numerical simulations are used to verify the effectiveness of the proposed strategies. The simulation results show that the proposed strategies can provide good dynamics control performance with less energy consumption.

Key words: **Over-actuated electric vehicles, dynamics control, energy efficiency optimisation, control allocation**

I. INTRODUCTION

With the combined challenge of energy optimisation and care for the environment, many studies have focused on the energy optimisation issue [1][2]. In particular, full electric vehicles with clean and efficient energy sources have the advantages of high fuel economy and zero carbon dioxide emissions. Electric vehicles can be driven by one centralised motor or by distributed motors in the wheels [3][4]. For electric vehicles with distributed motors in the wheels, also called electric vehicles with in-wheel motor, the transmission, differential and driving axle can be eliminated and mechanical loss can be largely reduced. Vehicle stability and handling is enhanced because of the rapid and precise independent control of the driving and steering torques of each wheel. In addition, in-wheel motors bring much flexibility to the vehicle design and the redundant actuators can be used to achieve multiple control targets. However, the number of motors and power electronics utilised and the increasing vehicle unsprung mass cause complexity in the control strategy of in-wheel-motor vehicles. Thus, the design of an effective control strategy for these electric vehicles needs to be focused.

Control allocation (CA) is an effective and widely applied method to control electric vehicles with in-wheel motor [5][6] and has been extensively studied [7]-[9]. In the current literature, the handling and stability control targets during vehicle combined longitudinal and lateral motion [10][11] and trajectory control [12][13][14][15] have been extensively focused. In addition to that, the energy-efficient control is also a highly important control target due to the limited energy on-board in these electric vehicles. Much research has been done to improve the energy efficiency from the point of view of motor design [16][17], motor control algorithms [18][19] and power electronics [20][21].

Based on the review of the current literature of the energy-efficient control, it can be seen that the energy-efficient control of electric vehicle can be mainly classified as the minimisation of the tyre friction loss and minimisation of the power consumption of electric motor. For instance, four objective functions for energy-efficient control are compared in [3]. These include: the minimisation of the total power output, the minimisation of the standard deviation

of individual tyre longitudinal slip ratio with respect to the average slip, the minimisation of the total longitudinal slip power loss and the minimisation of the average combined tyre force coefficient. In [22], it was also suggested that there was a variety of cost functions for energy-efficient CA optimisation which are related to the tyre slip, the actuator effort and power loss when the vehicle cornering motion was considered. In [23], three different motor types were demonstrated to achieve the reduction of the power loss by using an off-line procedure. We will narrow down our research scope into the energy-efficient control of electric driving motor since the steering motor has much less power consumption, and the tyre friction loss is not focused.

Energy-efficient control of the driving motor of electric vehicles during longitudinal motion has been proposed in the literature. Wang et al. proposed a longitudinal motion controller to improve the energy efficiency of the four in-wheel brushless DC (BLDC) motors by allocating different driving torques among the four motors in two different operation modes: the driving mode and the braking mode [24]. Gu et al. also proposed the energy-efficient control of the individual wheel driving motor for the longitudinal motion, and proved that equal distribution of all the driving torques can achieve optimal energy efficiency [25]. However, the in-wheel motor of a permanent magnetic synchronous motor (PMSM) was selected to be used in [25] and the motor efficiency map was different from the BLDC motor used in [24].

The above studies mainly focused on the energy-efficient CA of the vehicle during longitudinal motion, but the controller design will be more complex during combined longitudinal and lateral motion. Chen and Wang [26] considered the vehicle's longitudinal dynamics, lateral dynamics and yaw dynamics together. In their study, the planar motion controller had a two-layer structure. In the upper layer, the virtual control law is obtained by a dynamic sliding mode controller (SMC) in order to achieve robust control of the vehicle stability. In the lower level controller, the optimisation targets of the energy efficiency of driving motor and virtual control law in the upper level can be achieved by adaptive control. This whole control system, however, is based on the linear vehicle planer motion model, and the non-linear tyre characteristic, which is usually applicable in the high velocity and large steering angle situation, is neglected.

It can be found in the literature that the integrated control of vehicle dynamics and energy efficiency in the combined longitudinal and lateral motion based on the nonlinear vehicle dynamics model is less focused and this study can fill this research gap. In this study, as the redundant actuators can be used in the control system, the CA of the electric vehicle with in-wheel motor can achieve multiple control targets such as handling control, stability control and energy-efficient control. This allows the achievement of a proper trade-off strategy between each control target based on the comprehensive vehicle non-linear dynamics model.

In addition, the energy-efficient formulations defined in [24] are used in our study since these formulations can effectively present the characteristic of BLDC motor. However, it can be observed that this formulation is not continuous and the optimisation problem based on this formulation is not a convex problem, which may miss the global optimal point when solved by the conventional numerical optimisation algorithm, such as the interior-point method. In order to solve this problem, Chen and Wang [27] first applied the Karush-Kuhn-Tucker (KKT) algorithm to find all the local minima and the global optimal solution can be determined by comparing all the local minima and boundary values. This method can transfer the complex non-linear constrained optimisation problem into the classical eigenvalue problem. However, the simple first-order formulation of energy efficient coefficient η_i is applied in this study and the computational cost would significantly increase if the high-order formulation is used. Chen and Wang [26] later proposed the adaptive allocator to tackle this non-convex optimization problem with the fifth-order formulation of η_i, but the adaptive gains should be carefully tuned by very complex mathematic formulation and verification. In our study, the non-convex energy-efficient formation in [24] and fifth-order formulation of η_i are used to accurately present the motor energy efficiency and the proper optimisation algorithm should be chosen to find the global optimisation point.

The major contribution of this paper can be summarised as follows: in order to achieve the simultaneous dynamics control and energy efficiency optimisation, this paper first defines two criteria based on the tyre working region and the steering angle to categorise the vehicle motion status into linear pure longitudinal motion, linear cornering motion and non-linear cornering motion. Then for different motion status, different cost functions are developed. During the linear pure longitudinal motion and cornering motion, minimisation of the total driving power loss and the achievement of the desired dynamics performances are selected as the control targets with equal priorities. The optimisation cost function combines various dynamics control targets and energy-efficient control target, and the good trade-off performance between them can be achieved by adjusting the scaling factors of each control target term. In the non-linear cornering motion, the vehicle is very unstable and yaw rate and body slip angle are chosen as the primary targets because of the importance of vehicle handling and stability performance, while the energy efficiency is the secondary control target. The adaptive feedback proportional-integral-derivative (PID) controller based on the yaw rate and body slip angle control error is integrated into the optimal control allocator to guarantee the handling and stability control targets are achieved. In addition, due to discontinuous energy-efficient formulation and high-order energy-efficient coefficient representation in this study, the optimisation problem is a high-order non-convex constrained optimisation problem. To solve this problem, this study divides the whole discontinuous actuator constraint region into several continuous regions and the local optimal values can be easily determined in each continuous region by solving the convex constrained optimisation problem. After that, the global minima in the non-convex region can be found by comparing the local minima of each continuous region.

This paper is organised as follows. First the vehicle dynamics model of a four-wheel-steering (4WS) and four-wheel-driving

(4WD) electric vehicle is introduced. Then the proposed integrated energy-efficient control strategy is introduced. Finally, simulation examples are used to validate the effectiveness of the proposed control method.

II. Vehicle Dynamics Model

2.1 Vehicle dynamics model

In this paper, a 4WS and 4WD vehicle model is utilised to describe the dynamics motion of the electric vehicle with in-wheel steering and driving motors [28][29]. The equations of motion of this model are described as follows:

$$m\dot{v}_x = mv_y r + \left(F_{xfl} + F_{xfr} + F_{xrl} + F_{xrr}\right) \quad (1)$$

$$m\dot{v}_y = -mv_x r + \left(F_{yfl} + F_{yfr} + F_{yrl} + F_{yrr}\right) \quad (2)$$

$$I_z\dot{r} = l_f\left(F_{yfl} + F_{yfr}\right) - l_r\left(F_{yrl} + F_{yrr}\right) + \frac{b_f}{2}\left(F_{xfl} - F_{xfr}\right) + \frac{b_r}{2}\left(F_{xrl} - F_{xrr}\right) \quad (3)$$

where v_x, v_y, r are the vehicle longitudinal velocity, lateral velocity, and yaw rate, respectively. $F_{xfl}, F_{xfr}, F_{xrl}, F_{xrr}$ are the vehicle front left, front right, rear left and rear right longitudinal tyre forces, respectively, and $F_{yfl}, F_{yfr}, F_{yrl}, F_{yrr}$ are the vehicle front left, front right, rear left and rear right lateral tyre forces, respectively. l_f and l_r are the front and rear wheel base lengths, while b_f and b_r are the front and rear track widths. I_z and m are the moment of vehicle inertia in terms of yaw axis and vehicle mass. In order to simplify the vehicle model and improve computational efficiency, the vehicle roll dynamics are neglected in this study.

The tyre traction or brake force and side force are defined as F_{ti} and F_{si}, respectively, which can be related to the longitudinal and the lateral tyre forces by the steering angle δ_i as follows:

$$F_{xi} = F_{ti}\cos\delta_i - F_{si}\sin\delta_i \quad (4a)$$

$$F_{yi} = F_{ti}\sin\delta_i + F_{si}\cos\delta_i \quad (4b)$$

where $i = fl, fr, rl, rr$, which represents the front left, front right, rear left and rear right wheel, respectively. δ_i represents the steering angle of each vehicle wheel. It should be noted that all the steering angles mentioned in the paper indicate the steering angles of the vehicle wheels.

2.2 Vehicle tyre model

The non-linear Dugoff tyre model, which can well describe the non-linear tyre characteristic of combined longitudinal and lateral tyre force and the friction circle effect [30] is used in this study and described by:

$$\lambda_i = \frac{\mu F_{zi}(1 - s_i)}{2\sqrt{C_s^2 s_i^2 + C_\alpha^2 \tan^2\alpha_i}}$$

$$f(\lambda_i) = \begin{cases} \lambda_i(2 - \lambda_i) & (\lambda_i < 1) \\ 1 & (\lambda_i > 1) \end{cases}$$

$$F_{si} = \frac{C_\alpha \tan\alpha_i}{1 - s_i} f(\lambda_i)$$

$$F_{ti} = \frac{C_s s_i}{1 - s_i} f(\lambda_i) \quad (5)$$

where μ is the tyre-road friction coefficient. C_s is the longitudinal slip stiffness and C_α is the lateral cornering stiffness. s_i is the longitudinal slip ratio, and α_i is the lateral slip angle. ε_r is a constant value, and u_i is the vehicle velocity component in the wheel plane. F_{zi} is the vertical load of each wheel and the load transfer effect is considered, which can be calculated in [31].

2.3 Traction or brake dynamics model

Since one important feature of 4WD-4WS electric vehicles is the ability to perform independent traction or brake motion for each wheel, each wheel is integrated with an in-wheel traction or brake motor. The wheel rotation dynamics is described by the following equation:

$$I_\omega\dot{\omega}_i = -R_\omega F_{ti} + T_{di} \quad \text{during traction} \quad (6a)$$

$$I_\omega\dot{\omega}_i = -R_\omega F_{ti} - T_{bi} \quad \text{during braking} \quad (6b)$$

where I_ω is the wheel moment of inertia and ω_i is the angular velocity of each wheel. R_ω is the wheel radius and T_{di} is the traction torque of each wheel and T_{bi} is the brake torque of each wheel.

III. Integrated Dynamics Control and Energy Efficiency Optimisation

The 4WS-4WD electric vehicle has the advantage of redundant actuators which can be utilised to not only achieve the control goals of vehicle handling and stability, but can also realise the important goal of energy efficiency optimisation.

3.1 Motion status detection

Vehicles undertaking different motions are driven under different conditions and the control objectives for these will be different. For over-actuated electric vehicles, when the vehicle is undertaking a linear pure longitudinal motion and linear cornering motion, the dynamics performance and energy efficiency will both need to be considered. However, when the vehicle is undertaking lateral motion and the vehicle's tyre is working in the non-linear tyre region, the vehicle is in the condition of critical instability and handling and stability performance become the primary control targets. To deal with the different control objectives, different cost functions and control strategies will need to be developed. First of all, the threshold that determines the transition point between the linear pure longitudinal motion and the non-linear motion or turning motion must be defined. The following criteria are used to determine this transition point.

Criterion 1

According to the Dugoff tyre model used in this research (5), when $\lambda_i > 1$, the tyre is working in the linear tyre region. This condition can also be represented by following inequality:

$$\frac{\sqrt{(C_s s_i)^2 + (C_\alpha \tan\alpha)^2}}{1 - s_i} \leq \frac{1}{2}\mu F_{zi} \quad (7)$$

Criterion 2

In addition to working in the linear tyre region, the lateral acceleration of the vehicle in linear pure longitudinal motion must be small enough to ignore. The following equation suggests that the vehicle's lateral acceleration is related to the

input steering angle of the vehicle wheel and the longitudinal velocity:

$$\dot{v}_y = \frac{v_x^2}{Rg} = \frac{v_x^2 \delta}{g(l_f + l_r)} \tag{8}$$

where R is the vehicle turning radius, which is determined by the steering angle and vehicle base length. Thus, based on a group of experimental data, we assume that when the steering angle of the vehicle wheel is less than 0.02 rad, the vehicle lateral motion can be ignored.

3.2 Energy consumption model

For electric vehicles, the energy consumption models of the in-wheel driving motors are generally divided into two parts: pure energy consumption in driving mode and energy regeneration in braking mode based on the assumption that the energy can be partially re-gained through the regenerative braking function. The model which is widely used in the literature for the total power of in-wheel motors, P_m, can be described by the following equation by subtracting the total input power to the converter from the total output power of the battery [32].

$$P_m = \sum_{i=1}^{4} \frac{P_{Oi}}{\eta_{Oi}} + \sum_{i=1}^{4} \frac{1}{P_{Ii}\eta_{Ii}} \tag{9}$$

where P_{Oi} is the output power in the energy consuming mode and P_{Ii} is the input power in the energy gaining mode of the ith in-wheel motor, which are related to the driving torque T_{di}, braking torque T_{bi} and wheel angular velocity ω_i of the ith in-wheel motor as:

$$P_{Oi} = T_{di}\omega_i \tag{10a}$$

$$P_{Ii} = T_{bi}\omega_i \tag{10b}$$

where η_{Oi} is the output power efficiency in the energy consuming mode and η_{Ii} is the input power efficiency in the energy gaining mode of the ith in-wheel motor, which can be represented by the following relationships:

$$\eta_{Oi} = p_1 T_d^4 + p_2 T_d^3 + p_3 T_d^2 + p_4 T_d + p_5 \tag{11a}$$

$$\eta_{Ii} = p_6 T_b^3 + p_7 T_b^2 + p_8 T_b + p_9 \tag{11b}$$

where $p_1 - p_9$ are coefficients obtained by curve fitting of the actual experimental data from an in-wheel BLDC motor [32].

3.3 Control strategy for pure longitudinal motion control

When there is either little or no steering input applied and the tyre is working in the linear region according to Criterion 1 and Criterion 2, the pure longitudinal motion control mode is applied. In this case, only the vehicle longitudinal motion is considered and energy efficiency of driving motor power consumption is optimised. The cost function of CA problem can be represented as follows:

$$\min_{F_{xi}} J_1 = a_1\left(F_{xd}(k) - \sum_{i=1}^{4} F_{xi}(k)\right)^2 + a_2 P_m + a_3\left(F_{xi}(k) - F_{xi}(k-1)\right)^2 \tag{12a}$$

subject to:

$$-\frac{T_{bmax}}{R_\omega} \le F_{xi} \le \frac{T_{dmax}}{R_\omega} \tag{12b}$$

where a_1, a_2, a_3 are the scaling factors for the three optimisation terms. In order to achieve the best performance of the trade-off between each term, these scaling factors should be carefully tuned. k presents the value in current time step and $k-1$ presents the value in last time step. In this study, an in-wheel BLDC electric motor is applied. It has been suggested [32] that the maximum driving torque T_{dmax} is 100 N.m and the maximum regenerated brake torque T_{bmax} is 80 N.m. F_{xd} is the total desired longitudinal tyre force, which is determined according to the driver's input driving torque or brake torque. After the desired individual longitudinal tyre force F_{xi} is obtained, the individual driving or braking torque can be controlled to achieve the desired longitudinal tyre force using the following equations.

$$T_{di} = F_{xi} R_\omega \qquad F_{xi} \ge 0 \tag{13a}$$

$$T_{bi} = |F_{xi}| R_\omega \qquad F_{xi} < 0 \tag{13b}$$

The term P_m in the cost function (12) can be evaluated by inserting equations (9)-(11) and it is argued in [23] that the optimisation problem (12) is a non-convex problem because the term P_m includes the energy consumption mode and energy gaining mode. It is hard to calculate the analytical solution of the minimum value, so numerical algorithm is applied in this study. Traditional numerical algorithms, such as quadratic programming, active-set and fixed point method, can only achieve the local minima of a convex optimisation problem. To solve the non-convex optimisation problem in this study, the constraints of distributed individual driving torque in (12b) can be divided as the constraints [0,100] and [-80,0] and the whole constraints of four wheels can be divided as 16 constraints totally.

When the constraint has been divide, the term P_m only has one mathematic representation and becomes continuous in each divided constraint region. In this way, P_m is close to the convex function or at least has the global optimal value. The other two terms of the cost function (12a) are quadratic functions and are also convex. Therefore, the whole optimization problem (12) becomes close to convex problem. In each divided constraints, the optimisation problem (12) is a convex problem and it is easy to find the local minima. After that, the global minima can be obtained by comparing all the local minima.

It is noted that the third term in optimisation problem (12) tries to minimise the change of the distributed driving torque in last and current time step and guarantee the smooth allocation of driving torque. When the proposed integrated controller is working under the conditions of non-linear pure longitudinal motion, the control cost function (12) is still applied.

3.4 Control strategy for linear turning motion

Upper level

When the vehicle tyre is working in the linear tyre region but the driver's input steering angle is larger than the threshold value of *Criterion 2*, both the longitudinal, lateral and yaw motion should be considered. In addition, the energy efficiency of motor power consumption should be optimised. Thus the cost function of CA problem should be presented as follows:

$$\begin{aligned}\min_{F_{ti},F_{si}} & a_1 P_c + a_2\left(F_{xd}(k) - \cos\delta_{fl}(k-1)F_{tfl}(k) - \cos\delta_{fr}(k-1)F_{tfr}(k) - \cos\delta_{rl}(k-1)F_{trl}(k) - \cos\delta_{rr}(k-1)F_{trr}(k)\right)^2 + \\ & a_3\left(F_{yd}(k) - \cos\delta_{fl}(k-1)\,F_{sfl}(k) - \cos\delta_{fr}(k-1)\,F_{sfr}(k) - \cos\delta_{rl}(k-1)\,F_{srl}(k) - \cos\delta_{rr}(k-1)\,F_{srr}(k)\right) + a_4\Big(M_d(k) - \\ & \Big(l_f\left(F_{sfl}(k)\cos\delta_{fl}(k-1) + F_{sfr}(k)\cos\delta_{fr}(k-1)\right) - \\ & l_r(F_{srl}(k)\cos\delta_{rl}(k-1) + F_{srr}(k)\cos\delta_{rr}(k-1)) +\end{aligned}$$

$$\frac{b_f}{2}\left(-F_{sfl}(k)\sin\delta_{fl}(k-1)+F_{sfr}(k)\cos\delta_{fl}(k-1)\right)+\frac{b_r}{2}\left(-F_{srl}(k)\sin\delta_{rl}(k-1)+F_{srr}(k)\sin\delta_{rr}(k-1)\right)\Big)+a_5\left(F_{ti}(k)-F_{ti}(k-1)\right)^2+a_6\left(F_{si}(k)-F_{si}(k-1)\right)^2 \quad (14a)$$

subject to:

$$-\frac{T_{bmax}}{R_\omega}\le F_{ti}\le\frac{T_{dmax}}{R_\omega} \quad (14b)$$

$$F_{ti}^2+F_{si}^2\le\mu F_{zi}^2 \quad (14c)$$

Combing (14b) and (14c) and assuming $T_{dmax}>T_{bmax}$, the constraint (14c) can be rewritten as follows:

$$-\sqrt{\mu F_{zi}^2-\left(\frac{T_{dmax}}{R_\omega}\right)^2}\le F_{si}\le\sqrt{\mu F_{zi}^2-\left(\frac{T_{dmax}}{R_\omega}\right)^2} \quad (14c)$$

a_1-a_6 are scaling factors of each optimisation term, which need to be carefully tuned to achieve the best trade-off performance. a_1 is related to term of actuator energy efficiency. a_2-a_4 are terms of vehicle dynamics control targets and a_5-a_6 are used to minimise the change of distributed tyre force in the previous and current time step. The desired total longitudinal force F_{xd}, total lateral force F_{yd} and yaw moment M_d can be determined based on the desired yaw rate and slip angle as follows:

$$M_d=I_z\dot{r}_d \quad (15a)$$

$$F_{yd}=0 \quad (15b)$$

$$F_{xd}=\sum_{i=1}^{4}F_{xi}=\sum_{i=1}^{4}\frac{T_{di}-T_{bi}}{R_\omega} \quad (15c)$$

where r_d is the desired yaw rate, which can be calculated by as [29]. β_d is the desired vehicle body slip angle, of which value reflects the vehicle stability. The desired body slip angle is generally defined as zero ($\beta_d=0$) [29].

Similar to the last term in cost function (12), the last two terms in cost function (14) are trying to minimise the change of the distributed steering and driving actuators in the last and current time step.

The optimisation problem (14) is more complex than the pure longitudinal case and it is still a non-convex optimisation problem. In order to solve this non-convex optimisation problem, constraints (14b) and (14c) can be divided into 16 constraints according to driving or braking torques as given in Table 1. The optimisation problem is transferred into the convex problem when satisfying each divided constraint and the local minima can be found by traditional numerical algorithm. After that, the global minima can be determined by comparing every local minima.

Lower level

When the desired longitudinal and lateral tyre forces are determined in the upper level, the next problem is how to map the desired tyre forces into the actual steering angle and driving torque of each individual actuator.

Suzuki et al. used simple linear relationships between the steering angle, driving torque, side force F_{si}, and traction or brake force F_{ti} as followings [33]:

$$F_{sfl}=-C_a\left(\beta+\frac{l_f r}{v_x}-\delta_{fl}\right) \quad (16a)$$

$$F_{sfr}=-C_a\left(\beta+\frac{l_f r}{v_x}-\delta_{fr}\right) \quad (16b)$$

$$F_{srl}=-C_a\left(\beta-\frac{l_r r}{v_x}-\delta_{rl}\right) \quad (16c)$$

$$F_{srr}=-C_a\left(\beta-\frac{l_r r}{v_x}-\delta_{rr}\right) \quad (16d)$$

$$T_{di}=R_w F_{ti} \qquad F_{ti}\ge 0 \quad (17a)$$

$$T_{bi}=R_w|F_{ti}| \qquad F_{ti}<0 \quad (17b)$$

where β is the vehicle body slip angle. Based on (16)-(17), the actual steering angle and driving/braking torque can be obtained. The practical limitation of the steering angle is considered between -90 degrees and 90 degrees ($\delta_{max}=90$), which is larger than the traditional vehicle [34].

In the actual implementation of the proposed energy-efficient control method, a switch must be designed to achieve the smooth transition between the controllers under the pure longitudinal condition and under the cornering condition. Fuzzy logic method has been widely applied in the literature as the intelligent control method to control the nonlinear system with uncertainties [29][35]. In this study, a fuzzy logic controller is designed as this switch. The input of the fuzzy logic controller is the driver's input steering angle δ_f and the output is the scaling factor w between [0,1].

The fuzzy logic rule can be described as:

If input is S(small) then output is S; If input is B(big) then output is B.

Thus, the total distributed tyre force of individual wheel can be calculated as following:

$$F_{xi,total}=(1-w)F_{xi\_Lo}+wF_{xi\_La} \quad (18a)$$

$$F_{yi,total}=wF_{yi\_La} \quad (18b)$$

where F_{xi_Lo} is the distributed longitudinal force in the pure longitudinal condition and F_{xi_La} is the distributed longitudinal force in the turning motion. F_{yi_La} is the distributed lateral force in the turning condition.

3.5 Control strategy for non-linear turning motion

When the tyre of the vehicle is in the non-linear region and the vehicle is performing the turning motion, the vehicle is in the critical condition of instability. The control allocation strategy of the turning motion in equations (14)-(17) can only control the vehicle states when tyre is working in the linear tyre region. The distributed steering and driving actuators cannot accurately generate the desired tyre force when the tyre is working in the non-linear tyre region. This problem can be solved by measuring the actual tyre forces and using them as feedback information to adjust the control of the steering and driving actuators. As the tyre forces are difficult to measure in practice, the alternative feedback values of yaw rate and body slip angle are used instead in this paper. Although this alternative method has the problem of mapping from the yaw rate error and body slip angle error to the optimization control allocator, which is a time consuming and complex process, the advantage of this approach is that the control target of handling and stability performance can be directly and perfectly tracked and the computation speed of this approach is also fast enough to realise real-time control according to the simulation.

Thus, effective feedback controllers of the vehicle body slip angle and yaw rate are used to overcome the yaw rate control error and body slip angle control error caused by the non-linear tyre characteristic.

Specifically, the additional yaw moment will be calculated based on the feedback value of the yaw rate tracking error and

the additional lateral tyre force ΔF_y is calculated based on the lateral velocity error:

$$\Delta M_c = K_{1p}(r_d - r) + K_{1i}\int r_d - r + K_{1d}\frac{d(r_d - r)}{dt} \quad (19a)$$

$$\Delta F_y = K_{2p}\left(v_{yd} - v_y\right) + K_{2i}\int v_{yd} - v_y + K_{2d}\frac{d\left(v_{yd} - v_y\right)}{dt} \quad (19b)$$

where K_{1p}, K_{1i}, K_{1d} and K_{2p}, K_{2i}, K_{2d} are the proportional, integral and derivative feedback control gains. It is noted that the vehicle body slip angle is determined by lateral velocity, so lateral velocity response is considered to represent the body slip angle response in this study.

In order to tune the PID control gains in real-time, the adaptive law developed in [36] is applied to determine the K_{1p}, K_{1i}, K_{1d}.

The additionally controlled yaw moment ΔM_c and additionally controlled total lateral tyre force ΔF_y can be added into the desired yaw moment and desired total lateral tyre force in equation (15):

$$M_d = I_z\dot{r}_d + \Delta M_c \quad (20a)$$

$$F_{yd} = mv_x r_d + \Delta F_y \quad (20b)$$

In this way, the cost function (14) of the optimisation control allocator includes the yaw rate and body side-slip angle feedback error into the control target values in optimisation term and guarantee the yaw rate error and body slip angle can be minimised.

IV. Simulation Results

To test the dynamics performance of the suggested integrated dynamics control and energy efficiency optimisation method, numerical simulations are conducted under various conditions. In addition, the simulation results of traditional vehicle dynamics controller which has not considered the energy efficiency optimisation are also presented to compare with the proposed integrated method. The parameter values used in the simulations are listed in Table 1.

TABLE 1. PARAMETER VALUES USED IN SIMULATIONS [29].

m	Mass	1298.9 kg
l_f	Distance of c.g. from the front axle	1 m
l_r	Distance of c.g. from the rear axle	1.454 m
b_f	Front track width	1.436 m
b_r	Rear track width	1.436 m
C_s	Longitudinal stiffness of the tyre	50000 N/unit slip
I_z	Vehicle moment of inertial about yaw axle	1627 kgm^2
R_ω	Wheel radius	0.35 m
I_ω	Wheel moment of inertial	2.1 kgm^2
ε_r	Road adhesion reduction factor	0.015 s/m
C_α	Cornering stiffness of the tyre	30000 N/unit slip
a_1	Scaling factor of the lateral motion energy-efficient controller	1
a_2	Scaling factor of the lateral motion energy-efficient controller	1
h	height of the vehicle centre of gravity	0.533 m

4.1 Simulation results of pure longitudinal motion

In the first set of simulations, in order to effectively present the energy-efficient improvement of the proposed method, the widely used NEDC (New Europe Driving Cycle) vehicle test method is applied here. The tyre-road friction coefficient in all the three sets of simulations is assumed as 0.9. In the pure longitudinal motion, for the traditional dynamics control method, the control target is only the desired longitudinal velocity and the scaling factors of each term in (12) can be tuned as $a_1 = 0, a_2 = 2, a_3 = 1$. For the proposed integrated energy-efficient controller, the control targets are the desired longitudinal velocity and the energy consumption, and the scaling factors of each term in (12) can be tuned as $a_1 = 25, a_2 = 2, a_3 = 1$. The desired vehicle longitudinal velocity of NEDC is presented in Figure 1 and the actual longitudinal velocity control performances of the traditional dynamics control method and proposed integrated method are compared. In Figure 2, the total output power of electric motors of traditional dynamics method and proposed integrated method are also compared. The proposed integrated allocation method shows good trade-off performance of longitudinal velocity control and energy-efficient control. Compared with the traditional method in Figures 1 and 2, the proposed integrated method has much better motor power energy efficiency and similar longitudinal velocity control performance. The root mean square (RMS) values of the longitudinal velocity control error and energy consumption are shown in Table 2 to better present the good control performance of proposed integrated method. Figure 3 shows that the four driving torques are equally distributed for the traditional dynamics control method, which is widely used in the vehicle motion control. The proposed optimisation method, however, can change the equal torque distribution at peak values to achieve better energy-efficient performance.

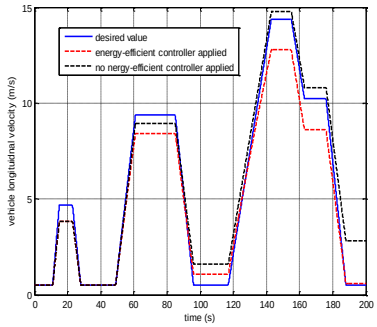

Figure 1. Longitudinal velocity in the simulation of linear pure longitudinal motion.

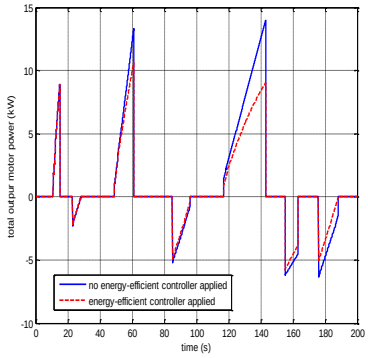

Figure 2. The total power consumption of driving motors in the simulation of linear pure longitudinal motion.

It should be noted that the torque distribution in Figure 4 is perfectly overlapped due to the same energy efficiency map applied. In the real situation, the individual driving motor may have slightly different energy efficiency maps even if the same types of motors are applied. This study, however, only shows the ideal conditions for theoretical analysis and this minor problem is not considered here.

4.2 Simulation results of vehicle cornering motion

Linear pure longitudinal motion is a simple control allocation scenario, and only the four driving/braking actuators are utilised and only the desired total longitudinal force need to be achieved. When the vehicle is cornering, the control targets of desired total longitudinal tyre force, total lateral tyre force and yaw moment must all be achieved. In addition to four driving/braking control actuators, four steering control actuators are used to achieve the control targets.

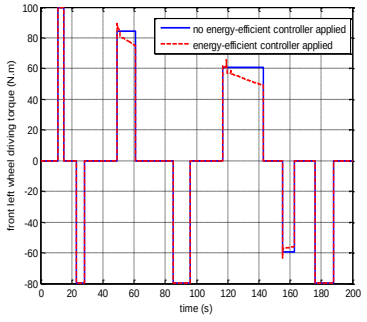

(a)

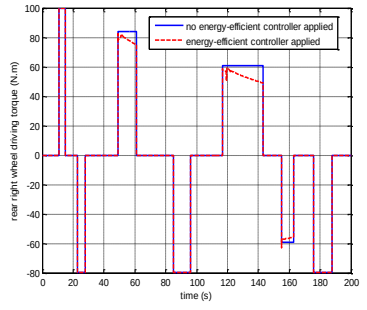

(b)

Figure 3. The distributed driving torque of the individual wheel in the linear pure longitudinal motion: (a) front left wheel (b) rear right wheel. (the front right and rear left wheel are not shown for the simplification)

In this set of simulations, the desired longitudinal velocity is still determined from NEDC driving test. In order to implement the combined longitudinal and lateral motion, the desired steering angle is designed to represent two sets of double lane change motion, which is shown in Figure 4.

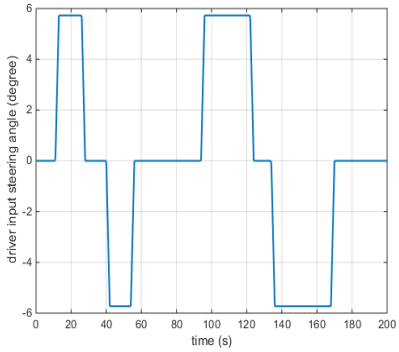

Figure 4. The desired input steering angle in the NEDC driving test in the cornering motion.

Figure 5 and Figure 6 present the control performance of the vehicle longitudinal velocity and lateral velocity of the traditional dynamics controller and proposed integrated energy-efficient controller. Figure 7 shows the total power consumption of driving motors of each method. For the integrated method, the scaling factors of each term in (14) can be tuned as $a_1 = 100, a_2 = a_3 = a_4 = 5, a_5 = a_6 = 0.05$. For the traditional method, the scaling factor of the term $a_1 = 0$. The proposed integrated method tries to balance the performances of various dynamics controls and energy efficiency, while the traditional dynamics controller only can achieve the best dynamics performance by neglecting the energy efficiency. Figures 5-7 prove that the integrated method, compared with the traditional dynamics control method, can achieve similar lateral velocity control performance and much better energy efficiency, although the longitudinal control performance is a little disadvantaged. The RMS values of dynamics control errors and energy consumption are also presented in Table 2 to further prove the good trade-off control performance of the proposed method. Figure 8 shows the actual allocated driving torque of each wheel and the driving torque allocated by traditional dynamics control method is oscillating more abruptly than the proposed integrated control method.

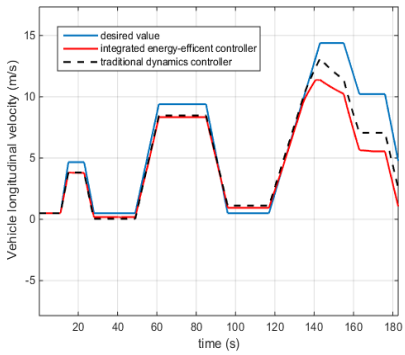

Figure 5. Vehicle longitudinal velocity in the cornering motion.

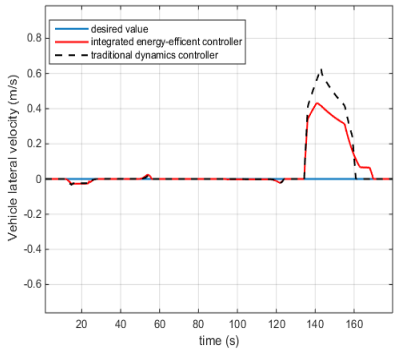

Figure 6. Vehicle lateral velocity in the cornering motion.

It is noted that from 10-30 seconds and 135-170 seconds, the large steering angle makes the vehicle tyre work in the non-linear tyre region and the vehicle is actually performing the non-linear cornering motion. The applied integrated energy-efficient controller cannot achieve the desired yaw rate and the proposed adaptive PID controller can be applied together with the energy-efficient controller to improve the dynamics control performance, which is presented in the next section.

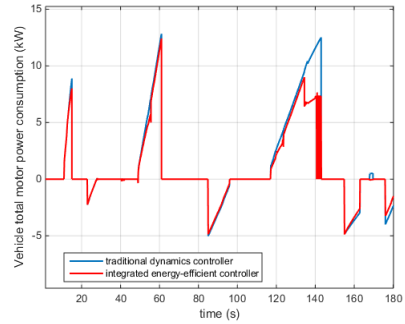

Figure 7. The total motor output power in the cornering motion.

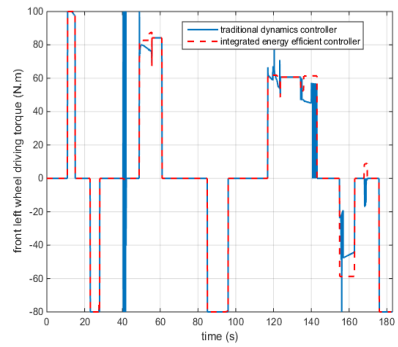

(a)

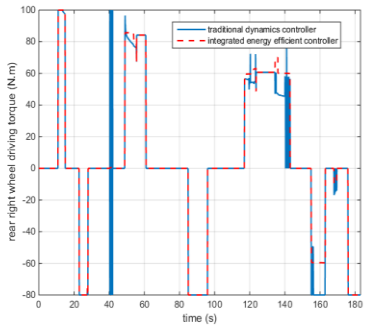

(b)

Figure 8. The distributed driving torque of the individual wheel in the cornering motion: (a) front left wheel (b) rear right wheel. (the front right and rear left wheel are not shown for the simplification)

4.3 Simulation results of vehicle non-linear cornering motion

In this section, the vehicle is assumed to drive in the non-linear cornering condition and the vehicle is very unstable because the tyre is working in the non-linear tyre region. Thus, the vehicle handling and stability are the primary control targets. The initial velocity is assumed as 10 m/s and the driver's steering input of double lane change is shown in Figure 9. The proposed adaptive PID feedback controller is included in the integrated energy-efficient controller in this set of simulations to improve the control performance of the primary control targets – yaw rate and body slip angle. It is also noted that the traditional numerical optimisation algorithm is applied in the first and second sets of simulations when the driving torque distribution is simple and regular. In this set of simulation, however, the driving torque distribution is irregular due to the complex turning condition. Thus, the proposed optimisation algorithm can achieve the global minima of the optimisation cost function and achieve better control performance. In Figures 10-12, the longitudinal velocity, lateral velocity and yaw rate control performance controlled by various methods and the total power consumption of various methods are compared. 'No feedback controller applied' means the proposed integrated energy-efficient controller is applied but the adaptive PID controller is not included; 'feedback controller applied' means the proposed integrated energy-efficient controller includes the adaptive PID controller; 'feedback controller + improved optimisation algorithm' means the proposed integrated energy-efficient controller includes the adaptive PID controller and the proposed improved optimisation algorithm, which can find the global minima, is also applied. Figure 10 shows that all the three methods can achieve similar control performance of longitudinal velocity. Figures 11 and 12 prove that the adaptive feedback PID controller can significantly improve the yaw rate and lateral velocity (body slip angle) control performance and guarantee the achievement of these primary control targets. In addition, the proposed fuzzy logic switch controller has been applied together with the PID feedback controller and the steady transition between the pure longitudinal motion with small steering angle and cornering motion with large steering angle can be achieved. Figure 13 shows that the motor power consumption is increased when the PID feedback controller is applied. This is reasonable since the additional control effort for the handling and stability control would consume more power. The proposed optimisation algorithm shows better energy-efficient performance compared with the traditional optimisation method. This is due to that the traditional optimisation method can only find the local minima and global minima can be missed out in the extreme non-linear condition. The RMS values of the longitudinal velocity control error, lateral velocity control error, yaw rate control error and total motor power consumption are presented in Table 2 to further verify

the above findings from the figures. Figure 14 also suggests that feedback PID controller requires more driving torque to be allocated and the distributed driving torque by the improved optimisation algorithm can better overcome the problem of oscillation compared with the traditional optimisation algorithm.

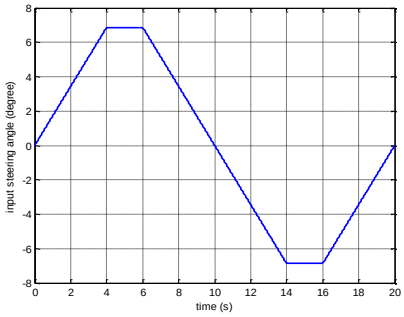

Figure 9. Driver's input steering angle in the non-linear cornering motion.

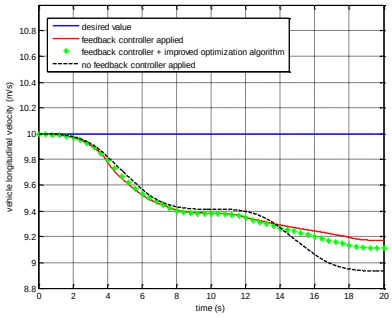

Figure 10. Vehicle longitudinal velocity in the non-linear cornering motion.

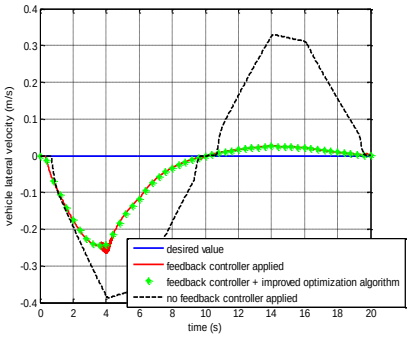

Figure 11. Vehicle lateral velocity in the non-linear cornering motion.

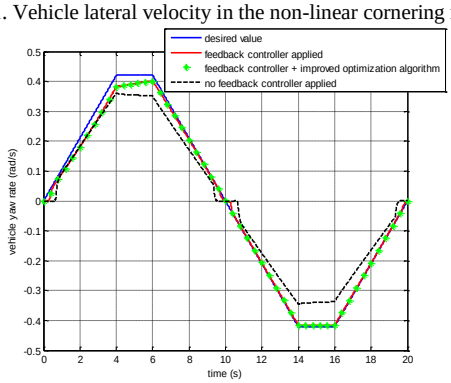

Figure 12. Vehicle yaw rate in the non-linear cornering motion.

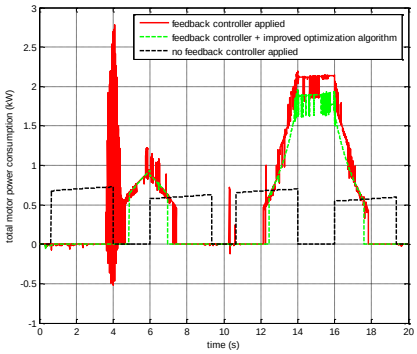

Figure 13. Total motor power consumption in the non-linear cornering motion.

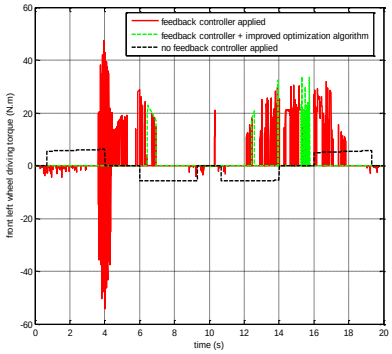

(a)

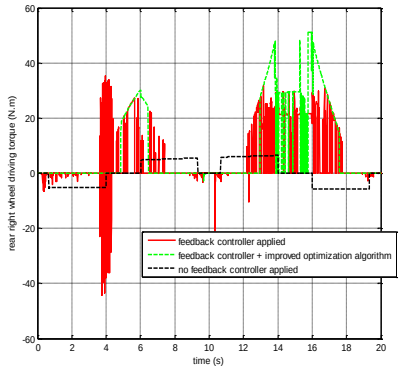

(b)

Figure 14. The distributed driving torque of the individual wheel in the non-linear cornering motion: (a) front left wheel (b) rear right wheel. (the front right and rear left wheel are not shown for the simplification)

Table 2. RMS value of the dynamics control error and motor power consumption

Vehicle moving scenarios		Longitudinal velocity control error (m/s)	Lateral velocity control error (m/s)	Yaw rate error (rad/s)	Motor driving power loss (kW)
Pure longitudinal motion	Traditional dynamics controller applied	0.8878	N/A	N/A	4.0994
	Integrated energy-efficient controller applied	0.8731	N/A	N/A	3.1626
Combined longitudinal motion and cornering motion	Traditional dynamics controller applied	1.4259	0.1800	0.0569	3.9150
	Integrated energy-efficient controller applied	2.0366	0.1306	0.0677	3.1669

Non-linear cornering motion	Integrated energy-efficient controller applied	0.6575	0.2377	0.0524	0.5236
	Integrated energy-efficient controller +feedback controller	0.5904	0.1007	0.0168	0.9187
	Integrated energy-efficient controller + feedback controller + improved optimization algorithm	0.6109	0.1001	0.0168	0.7762

V. CONCLUSION

This study proposes an integrated dynamics control and energy efficiency optimisation method for linear pure longitudinal motion, linear turning motion, and non-linear turning motion. According to the simulation results, our findings can be summarised as follows:

In linear pure longitudinal motion and linear cornering motion, the simulation results suggest that the proposed integrated energy-efficient control allocator can achieve better trade-off between the dynamics control targets and the energy-efficient control target compared with the traditional dynamics control allocation method.

In the non-linear cornering motion, the proposed adaptive PID feedback controller can achieve much better control performance of the primary control targets: yaw rate and body slip angle. The control allocator optimised by the proposed improved optimisation algorithm can achieve better energy-efficient control performance due to that the traditional optimisation method can only find the local minima and global minima can be missed out in the extreme non-linear condition.

The proposed motion detection criteria are proved to successfully determine the transition point between the linear pure longitudinal motion and the cornering motion, and the control strategies can be switched by a designed fuzzy logic switch controller at this transition point.

In the future, the proposed integrated control allocation method will be tested on a real electric vehicle with in-wheel steering and in-wheel driving in both longitudinal motion and lateral motion.

ACKNOWLEDGEMENTS:

This research was supported under Australian Research Council's Discovery Projects funding scheme (project number DP140100303) and the Open Research Fund Program of the State Key Laboratory of Advanced Design and Manufacturing for Vehicle Body, Hunan University (31515001).

References

[1] Yin, C., Chen, Y. and Zhong, S.M., "Fractional-order sliding mode based extremum seeking control of a class of non-linear systems", *Automatica*, vol.50, no.12, pp.3173-3181, 2014.

[2] Yin, C., Dadras, S., Huang, X., Mei, J., Malek, H., and Cheng, Y., "Energy-saving control strategy for lighting system based on multivariate extremum seeking with Newton algorithm", *Energy Conversion and Management*, vol.142, pp.504-522, 2017.

[3] De Novellis, L., Sorniotti, A., and Gruber, P., "Wheel torque distribution criteria for electric vehicles with torque-vectoring differentials", *IEEE Transactions on Vehicular Technology*, vol.63, no.4, pp.1593-1602, 2014.

[4] Liu, H., Chen, X., and Wang, X., "Overview and prospects on distributed drive electric vehicles and its energy saving strategy", *Przegląd Elektrotechniczny*, vol.88, pp.122-125, 2012.

[5] Oppenheimer, M., Doman, D., and Bolender, M., *Control allocation*, in W. S. Levine, ed., "The Control Handbook, Control System Applications, Second Edition", chapter 8.

[6] Fossen, T.I., and Johansen, T.A., "A survey of control allocation methods for ships and underwater vehicles", *14th Mediterranean Conference on Control and automation*, Ancona, 2006.

[7] Wang, J., and Longoria, R.G., "Coordinated and reconfigurable vehicle dynamics control", *IEEE Trans. Control Syst. Technol.*, vol.17, no.3, pp. 723-732, May 2009.

[8] Plumlee, J.H., Bevly, D.M., and Hodel, A.S., "Control of a ground vehicle using quadratic programming based control allocation techniques", in *Proc. 2004 Amer. Control Conf.*, 2004, pp. 4704-4709.

[9] Tjønnås, J., and Johansen, T.A., "Stabilization of automotive vehicle using active steering and adaptive brake control allocation", *IEEE Transactions on Control Systems Technology*, vol.18, no.3, pp.545-558, 2010.

[10] Powell, B.K., Bailey, K.E. and Cikanek, S.R., "Dynamic modeling and control of hybrid electric vehicle powertrain systems", *IEEE Control Systems*, vol.18, no.5, pp.17-33, 1998.

[11] Pham, H., Hedrick, K. and Tomizuka, M., "Combined lateral and longitudinal control of vehicles for IVHS", *American Control Conference*, pp.1205-1206, 1994.

[12] Dadras, S., "Path Tracking Using Fractional Order Extremum Seeking Controller for Autonomous Ground Vehicle", *SAE Technical Paper*, No. 2017-01-0094, 2017.

[13] Fritz, H., "Longitudinal and lateral control of heavy duty trucks for automated vehicle following in mixed traffic: experimental results from the CHAUFFEUR project", *Proceedings of the 1999 IEEE International Conference* in Control Applications, pp. 1348-1352, 1999.

[14] Dadras, S., Momeni, H.R. and Dadras, S., "Adaptive control for ship roll motion with fully unknown parameters", *IEEE International Conference on Control and Automation*, pp. 270-274, 2009.

[15] Zhao, R.C., Wong, P.K., Xie, Z.C. and Zhao, J., "Real-time weighted multi-objective model predictive controller for adaptive cruise control systems", *International Journal of Automotive Technology*, vol.18, no.2, pp.279-292, 2017.

[16] Fang, L., Jung, J., Hong, J. and Lee, J., "Study on high-efficiency performance in interior permanent magnet synchronous motor with double-layer PM design", *IEEE Trans. Magnetics*, vol.44, no.11, pp.4393-4396.

[17] Cvetkovski, G., and Petkovska, L., "Efficiency maximisation in structural design optimization of permanent magnet synchronous motor", *Proc. 18th Int. Conf. Electrical Machines*, 2008.

[18] Morimoto, S., Tong, Y., Takeda, Y., and Hirasa, T., "Less minimization control of permanent magnet synchronous motor drives", *IEEE Trans. Industrial Electronics*, vol.41, no.5, pp.511-517, 1994.

[19] Cavallaro, C., Ditommaso, A. O., Miceli, R., Raciti, A., Galluzzo, G. R. and Trapanese, M., "Efficiency enhancement of permanent-magnet synchronous motor drives by online loss minimization approaches", *IEEE Trans. Industrial Electronics*, vol.52, no.4, pp.1153-1160, 2005.

[20] Wai, R., Duan, R., Lee, J., and Liu, L., "High efficiency fuel-cell power inverter with soft-switching resonant technique", *IEEE Trans. Energy Conversion*, vol.20, no.2, pp.485-492, 2005.

[21] Lai, J. S., Yong, R. W., Ott Jr., G. W., and McKeever, J. W., "Efficiency modelling and evaluation of a resonant snubber based soft-switching inverter for motor drive applications", *Proc. 26th Annual IEEE Power Electronics Specialists Conf.*, vol.2, pp.943-949.

[22] Pennycott, A., De Novellis, L., Sabbatini, A., Gruber, P., and Sorniotti, A., "Reducing the motor power losses of a four-wheel drive, fully electric vehicle via wheel torque allocation", *Proc IMechE Part D: J Automobile Engineering*, vol.228, no.7, pp.830-839, 2014.

[23] Pennycott, A., De Novellis, L., Gruber, P., and Sorniotti, A., "Enhancing the energy efficiency of fully electric vehicles via the minimization of motor power loss", in *IEEE International Conference on Systems, Man, and Cybernetics*, Manchester, UK, 2012.

[24] Wang, R., Chen, Y., Feng, D., Huang, X., and Wang, J., "Development and performance characterization of an electric ground vehicle with independently actuated in-wheel motors", *J. Power Sources*, vol.196, no.8, pp.3962-3971.

[25] Gu, J., Ouyang, M., Lu, D., Li, J., and Lu, L., "Energy efficiency optimization of electric vehicle driven by in-wheel motors", *International Journal of Automotive Technology*, vol.14, no.5, pp.763-772, 2013.
[26] Chen, Y. and Wang, J., "Adaptive energy-efficient control allocation for planar motion control of over-actuated electric ground vehicles", *IEEE Transactions on Control System Technology*, vol.22, no.4, 2014.
[27] Chen, Y. and Wang, J., "Fast and global optimal energy-efficient control allocation with applications to over-actuated electric ground vehicles", *IEEE Transactions on Control Systems Technology*, vol.20, no.5, pp.1202-1211, 2012.
[28] Li, B.Y., Li, W.H., Kennedy, O., and Du, H.P., "The dynamics analysis of an omni-directional vehicle," *International Journal of Automotive Technology*, vol.15, no.3, pp.387-398, 2014.
[29] Boada, B., Boada, M. and Díaz, V., "Fuzzy-logic applied to yaw moment control for vehicle stability," *Vehicle System Dynamics*, vol.43, pp.753-770, 2005.
[30] Dugoff, H., Fancher, P.S. and Segel, L., 1970, "An analysis of tyre traction properties and their influence on vehicle dynamic performance", *SAE 700377*, pp. 1219-1243.
[31] Zhao, Y., and Zhang, J., "Yaw stability control of a four-independent-wheel drive electric vehicle", *Int. J. Electric and Hybrid Vehicles*, vol.2, no.1, pp.64-76, 2009.
[32] Chen, Y., and Wang, J., "Design and experimental evaluations on energy efficient control allocation methods for overactuated electric vehicles: Longitudinal motion case", *IEEE Transactions on Mechatronics*, vol.19, no.2, pp.538-548, 2014.
[33] Suzuki, Y., Kano, Y., and Abe, M., "A study on tyre force distribution controls for full drive-by-wire electric vehicle", *Vehicle System Dynamics*, DOI: 10.1080/00423114.2014.894198.
[34] Best, M., "Identifying tyre models directly from vehicle test data using an extended Kalman filter," *Vehicle System Dynamics*, vol.48, pp.171-187, 2010.
[35] Tahami, F., Farhangi, S. and Kazemi, R., "A fuzzy logic direct yaw-moment control system for all-wheel-drive electric vehicles," *Vehicle System Dynamics*, vol.41, no.3, pp.203-221, 2004.
[36] Chang, W., Hwang, R., and Hsieh, J., 'A self-turning PID control for a class of non-linear systems based on the Lyapunov approach', *Journal of Process Control*, 2002, vol.12, pp.233-242.